Molecular Crystals and Liquid Crystals

ISSN: 1542-1406 (Print) 1563-5287 (Online) Journal homepage: http://www.tandfonline.com/loi/gmcl20

Synthesis, characterization, and antibacterial activity of 6-Chloro-8-methyl-2-oxo-2H-chromene-3-carboxylic acid ethyl ester

N. Latha Rani, T. Prashanth, M. A. Sridhar, H. D. Gurupadaswamy, K. Shaukath Ara & N. K. Lokanath

To cite this article: N. Latha Rani, T. Prashanth, M. A. Sridhar, H. D. Gurupadaswamy, K. Shaukath Ara & N. K. Lokanath (2016) Synthesis, characterization, and antibacterial activity of 6-Chloro-8-methyl-2-oxo-2H-chromene-3-carboxylic acid ethyl ester, Molecular Crystals and Liquid Crystals, 624:1, 262-270, DOI: 10.1080/15421406.2015.1038032

To link to this article: http://dx.doi.org/10.1080/15421406.2015.1038032

MOL. CRYST. LIQ. CRYST.
2016, VOL. 624, NO. 1, 262–270
http://dx.doi.org/10.1080/15421406.2015.1038032

Taylor & Francis
Taylor & Francis Group

Synthesis, characterization, and antibacterial activity of 6-Chloro-8-methyl-2-oxo-2H-chromene-3-carboxylic acid ethyl ester

N. Latha Rani[a], T. Prashanth[b], M. A. Sridhar[a], H. D. Gurupadaswamy[b], K. Shaukath Ara[b], and N. K. Lokanath[a]

[a]Department of Studies in Physics, University of Mysore, Manasagangotri, Mysuru, India; [b]Department of Chemistry, Yuvaraja's College (Autonomous), University of Mysore, Mysuru, India

ABSTRACT

The title compound was synthesized by reacting 2-hydroxy-4-methoxybenzaldehyde with diethyl malonate in the presence of piperidine catalyst and ethanol as solvent. The chemical structure of the title compound was elucidated by elemental analysis, ^{1}H-NMR, and IR. The crystal structure was determined by X-ray diffraction data. It crystallizes in monoclinic crystal system, $P2_1/c$ space group with unit cell parameters, a = 12.840(2) Å, b = 24.790(4) Å, c = 7.8544(13) Å, β = 98.035(5)°, V = 2475.5(7) Å^3, and Z = 8. The molecular and crystal structure of the title compound is stabilized by inter- and intramolecular interactions of the type C—H···O. The newly synthesized compound was screened for its antibacterial activity against two gram-positive and two gram-negative bacteria.

KEYWORDS

Antibacterial activity; Bacillus cereus; Coumarin; phytochemical Pseudomonas aeruginosa; Salmonella typhimurium; Staphylococcus aureus

Introduction

The title compound is a coumarin derivative. Coumarin is a natural substance found in many plants. It is a phytochemical with a vanilla-like flavor. The synthesis of coumarins and their derivatives have attracted considerable attention from organic and medicinal chemists for many years as a large number of natural and synthetic products. Some of them show clinical value toward breast cancer, leukemia, tumor cells, etc. A few possess potent antiviral activities [1].

Introducing halogen to the coumarin derivatives helps in enhancing the antimicrobial activity [2,3]. It has been reported that chlorine-substituted 4-hydroxycoumarin derivative has potent anticoagulant activity [4].

Herein, we report the synthesis, characterization, and crystal structure of the title compound. The newly synthesized compound was screened for its antibacterial activity.

CONTACT M. A. Sridhar mas@physics.uni-mysore.ac.in Department of Studies in Physics, University of Mysore, Manasagangotri, Mysuru 570 006, India.
Color versions of one or more of the figures in the article can be found online at www.tandfonline.com/gmcl.

Experimental section

Materials and methods

Chemicals were purchased from Sigma Aldrich Chemical Corporation. Thin Layer Chromatography (TLC) was performed on an aluminum-backed silica plates from Merck & Co., and visualized under UV-light. Melting points were determined on a Thomas Hoover capillary melting point apparatus with a digital thermometer. IR spectra were recorded on Perkin-Elmer spectrophotometer version 10.03.09, ^{1}H NMR spectra were recorded on a Bruker 400 MHz NMR spectrophotometer in DMSO-d_6 solvent and the chemical shifts were recorded in δ (ppm) downfield from tetramethylsilane. Elemental analysis was done by Perkin-Elmer 2400 elemental analyzer and results are within 0.4% of the calculated value.

Synthesis of 6-Chloro-8-methyl-2-oxo-2H-chromene-3-carboxylic acid ethyl ester

6-Chloro-8-methyl-2-oxo-2H-chromene-3-carboxylic acid ethyl ester was synthesized from 2-Hydroxy-4-methoxy-benzaldehyde (0.0187 mol) and diethyl malonate (0.0188 mol) in the presence of 0.1 mL of piperidine as a catalyst and ethanol as solvent. The reaction mixture was refluxed for 8 hr and the reaction was monitored by TLC using benzene:ethyl acetate (4:1) as an eluent. The reaction mixture was allowed to cool to room temperature, then the reaction mass was quenched in to ice cold water and the solid obtained was filtered to obtain compound in good yield (90%), m.p. 140°C–142°C (Scheme 1).

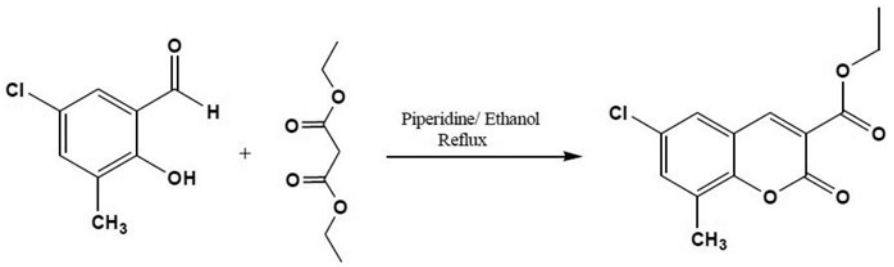

Scheme 1. Scheme of 6-Chloro-8-methyl-2-oxo-2H-chromene-3-carboxylic acid ethyl ester.

In vitro antibacterial activity

In view of the biological importance of different series of coumarin derivatives, the synthesized title compound was screened for its antibacterial activity.

Antibacterial assays were carried out at Department of Studies in Microbiology, University of Mysore, Mysuru. The compound was screened for antibacterial activity against two gram-positive bacteria namely *Bacillus cereus* [MTCC (Microbial Type Culture Collection) No. 1272], *Staphylococcus aureus* (MTCC No. 7443), and two gram-negative bacteria, namely *Pseudomonas aeruginosa* (MTCC No. 7093) and *Salmonella typhimurium* (MTCC No. 733). The bacterial strains were inoculated in nutrient broth, and kept for overnight culture at 37°C.

The MIC is defined as the minimum inhibitory concentration able to inhibit any visible bacterial growth. Antibacterial activity was determined by broth microdilution method performed in 96 well microtiter plate, using 2,3,5-triphenyl tetrazolium chloride (TTC) as an indicator for bacterial growth [5], by dissolving 5 mg of sample in 1 mL of ethanol solvent.

Table 1. Elemental analysis of the title compound.

Element	Element Experimental (%)	Calculated (%)
Carbon	58.55	58.57
Hydrogen	4.16	4.13

For susceptibility testing, 100 μL of nutrient broth was distributed from first to eighth, and tenth to twelfth test wells. Approximately 100 μL of compound initially dissolved in ethanol was distributed to first well, from which 100 μL was taken and transferred till the concentration reached 0.39×10^{-2} mg mL^{-1}. Tenth and eleventh wells served as negative and positive (gentamicin) controls, respectively; twelfth well was a sterility control. Later 50 μL of the final bacterial inoculum was added to the appropriate wells.

The concentrations of the prepared solutions were as follows: 0.5 mg mL^{-1}, 0.25 mg mL^{-1}, 0.125 mg mL^{-1}, 0.625×10^{-1} mg mL^{-1}, 0.3125×10^{-1} mg mL^{-1}, 0.156×10^{-1} mg mL^{-1}, 0.78×10^{-2} mg mL^{-1}, 0.39×10^{-2} mg mL^{-1}.

Inoculated plates were incubated at 37°C for 24 hr. One hour before the end of incubation, 10 μL of TTC was added to the wells and the plates were incubated for another hour. The lowest concentration of each well showing no visible growth was recorded as the MIC [6]. The optical density of the plate was measured at 600 nm on ELISA reader of Thermo Scientific.

Results and discussion

Elemental analysis

In order to confirm the chemical composition of the synthesized compound, carbon (C) and hydrogen (H) analysis was carried out. The experimental and calculated percentages of C and H are given in Table 1. The differences between experimental and calculated percentages of C and H were very small and are within the experimental errors. This confirmed the formation of the product in the stoichiometric proportion.

FT-IR spectral analysis

The Fourier transform infrared spectroscopy (FT-IR) spectrum of the crystal structure is shown in Fig. 1. The peak at 3067 cm^{-1} was in correspondence to the C—H stretching of the

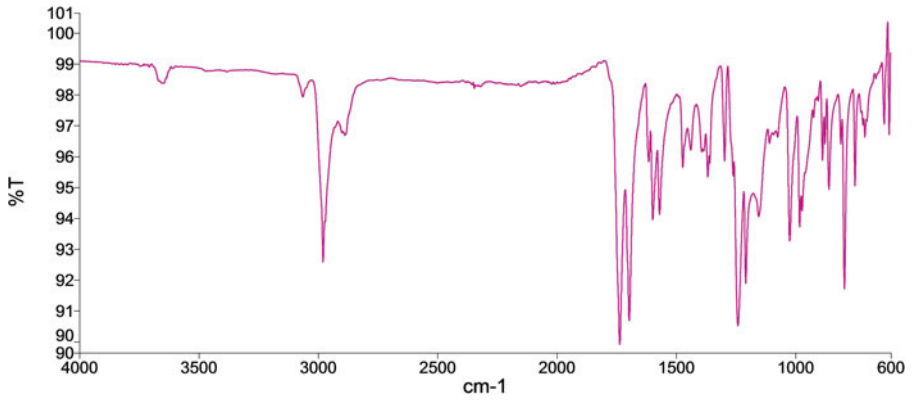

Figure 1. FTIR spectrum of title compound.

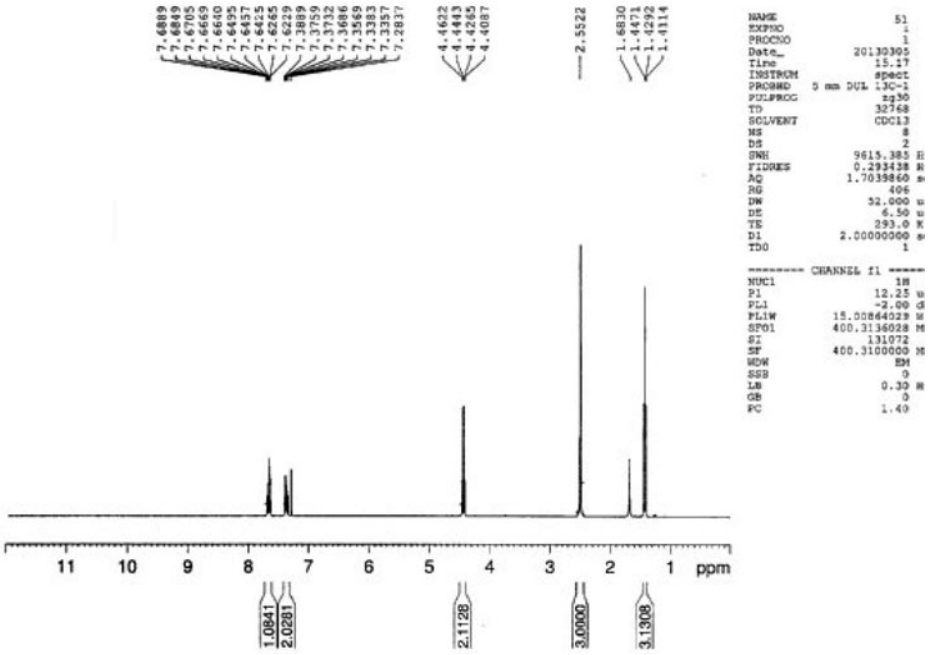

Figure 2. [1]H NMR spectra of the title compound.

aromatic protons. The peaks observed at 1736 cm^{-1} is assigned to the C=O of ethyl ester, and the peak at 1614 cm^{-1} is for C=O stretching vibration of coumarin. The peak at 1260 cm^{-1} is assigned for the C–O stretching.

NMR spectral analysis

The spectrum [1]H NMR of the crystal structure is shown in Fig. 2. The NMR peak at δ 1.4 (t, $J = 6.6$ Hz, 3H) is for three hydrogens in CH_3 of ester, the singlet peak at δ 2.5 is for the methyl group attached to the aromatic ring, the peak at δ 4.4 (q, $J = 5.9$ Hz, 2H), is for two hydrogens of $COOCH_2$, and the peaks at δ 7.3–7.7 (m, 3 Ar-H) clearly indicates the three aromatic hydrogens of the compound, thus, confirms the structure.

X-ray crystal structure determination

A white transparent single crystal of the title compound with approximate dimensions 0.18 × 0.18 × 0.18 mm was used for structural analysis using X-ray diffraction technique. Data were collected on a Bruker CCD diffractometer equipped with Cu $K\alpha$ radiation. Data reduction of all the measured reflections and absorption corrections were carried out using the *APEX 2* package [7]. Crystal structure was solved by direct methods using *SHELXS-97* and refined by full-matrix least squares refinement against F^2 using *SHELXL-97* [8]. All non-hydrogen atoms were refined anisotropically and hydrogen atoms were placed in chemically acceptable positions.

The title compound $C_{13}H_{11}ClO_4$ crystallizes in monoclinic crystal system, with $P2_1/c$ space group. The unit cell parameters $a = 12.840(2)$ Å, $b = 24.790(4)$ Å, $c = 7.8544(13)$ Å, $\beta =$

Table 2. The crystal data and structure refinement details.

CCDC Deposit Number	10,16,849
Empirical formula	$C_{13}H_{11}ClO_4$
Formula weight	266.67
Temperature	296 K
Wavelength	1.54178 Å
Crystal system	Monoclinic
Space group	P21/c
Cell dimensions	$a = 12.840(2)$ Å, $c = 7.8544(13)$ Å
	$b = 24.790(4)$ Å, $\beta = 98.035(5)°$
Volume	2475.5(7) Å^3
Z	8
Density(calculated)	1.431 Mg m^{-3}
Absorption coefficient	2.789 mm^{-1}
F000	1104
Crystal size	0.18 × 0.18 × 0.18 mm
θ range for data collection	6.39°–65.05°
Index ranges	$-13 \le h \le 15$
	$-25 \le k \le 29$
	$-8 \le l \le 5$
Reflections collected	9556
Independent reflections	3802
Refinement method	Full matrix least-squares on F^2
Data/restraints/parameters	3802/0/329
Goodness-of-fit on F^2	1.081
Final [$I > 2\sigma(I)$]	$R1 = 0.0489$, $wR2 = 0.1403$
Largest diff. peak and hole	0.255 and −0.260 eÅ−3

98.035(5)°, $V = 2475.5(7)$ Å^3, and $Z = 8$. The crystal data and structure refinement details are given in Table 2.

The geometrical calculations were carried out using the program *PLATON* [9]. The molecular and packing diagrams were generated using *Mercury* [10].

The asymmetric unit consists of two molecules. Figures 3 and 4 show the *ORTEP* diagrams of the molecules A and B, respectively. The bond distances and angles are listed in the Table 3. Torsion angles are listed in the Table 4. Hydrogen-bond geometry is given in Table 5. The molecular structure of the title compound $C_{13}H_{11}ClO_4$ consists of 2H-chromene with carboxylic acid ethyl ester substituted at the third position. The chlorine moiety is attached at the sixth position. The methyl group is at the eighth position. The 2H-chromene ring is planar [r.m.s. deviation 0.068(2) Å], with a maximum deviation of 0.099(2) Å for C(10A) in molecule A and [r.m.s. deviation 0.02(2) Å], with a maximum deviation of 0.029(2) Å for C(10B) in molecule B.

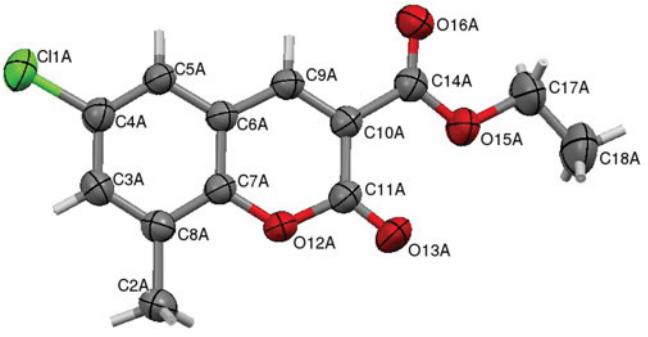

Figure 3. The *ORTEP* diagram of molecule A of the title compound with 50% probability.

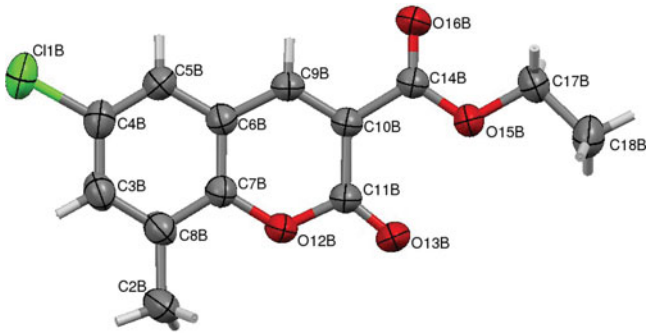

Figure 4. The *ORTEP* diagram of molecule B of the title compound with 50% probability.

Table 3. Selected bond lengths and bond angles (Å, deg.).

Atoms	Distances	Atoms	Angles
Cl1A-C4A	1.737 (2)	O12A-C11A-O13A	115.9 (2)
Cl1B-C4B	1.735 (2)	O13A-C11A-C10A	127.7 (2)
O12A-C11A	1.376 (3)	O12A-C7A-C8A	116.85 (18)
O12A-C7A	1.368 (3)	C5A-C6A-C9A	123.11 (19)
O13A-C11A	1.196 (3)	O13A-C11A-C10A	127.7 (2)
O15A-C14A	1.321 (3)	O12B-C11B-O13B	115.65 (18)
O15A-C17A	1.457 (4)	O13B-C11B-C10B	128.2 (2)
O16A-C14A	1.197 (3)	O12B-C7B-C6B	120.62 (19)
O13B-C11B	1.193 (3)	O16A-C14A-C10A	122.9 (2)
O12B-C7B	1.370 (3)	O13B-C11B-C10B	128.2 (2)

Table 4. Selected torsion angles (deg.).

Atoms	Angle	Atoms	Angle
C7A-O12A-C11A-C10A	−7.5 (3)	C14A-C10A-C11A-O13A	10.7 (4)
C11A-O12A-C7A-C8A	178.0 (2)	C11B-C10B-C14B-O16B	174.9 (2)
C7A-O12A-C11A-O13A	171.9 (2)	C9A-C10A-C14A-O16A	10.8 (4)
C11A-O12A-C7A-C6A	−1.8 (3)	C9A-C10A-C11A-O13A	−167.8 (3)
C14A-O15A-C17A-C18A	176.0 (3)	C11A-C10A-C14A-O15A	13.2 (3)
C17A-O15A-C14A-O16A	0.5 (4)	C11A-C10A-C14A-O16A	−167.7 (2)
C7B-O12B-C11B-O13B	−178.8 (2)	C8B-C3B-C4B-C5B	−1.2 (4)
C17B-O15B-C14B-O16B	−0.4 (3)	Cl1B-C4B-C5B-C6B	179.79 (18)
C14B-O15B-C17B-C18B	174.7 (2)	C3B-C4B-C5B-C6B	0.8 (4)

The bond lengths and angles are in fairly good agreement with those of previously reported coumarin derivatives. The bond length of C=O attached to the pyrone moiety in molecules A and B are, respectively, 1.196(3) Å and 1.193(3) Å which are greater than the corresponding values of 1.188(2) Å and 1.189(4) Å reported for C_{12} H_9 Cl O_4 and C_{12} H_9 Br O_4, respectively [11]; lesser than the corresponding value of 1.203(2) Å reported for Cinnamyl 2-oxo-2H-chromene-3-carboxylate [12].

The 10-membered rings of 2H-chromene (O12-C7-C8-C3-C4-C5-C6-C9-C10-C11) of molecules A and B are *sp2* hybridized. They are well described by the torsion angles 111.39° and 117.92°, respectively; which suggest that they adopt anticlinal conformations, with the puckering amplitudes 0.181(2) Å and 0.053(2) Å, respectively.

The bond angle O12-C11-O13 in molecules A and B are 115.9(2)° and 115.65(18)° which are less than 127.7(2)° and 128.2(2)°, respectively, for O13-C11-C10 of molecules A and B. This can be ascribed to the steric effect. The bond angles at the junctions of phenyl and pyrone rings of 2H-chromene are 116.85(18)° and 116.97(19)° for O12-C7-C8;

Table 5. Hydrogen-bond geometry (Å, deg.).

D—H···A	D—H	H···A	D···A	D—H···A
C2A – H2A2 · · · O13B [(a)]	0.96	2.54	3.392 (4)	148
C3A – H3A · · · O13B [(a)]	0.93	2.38	3.243 (3)	155
C2B – H2B1 · · · O13A [(b)]	0.96	2.42	3.351 (3)	163
C5A – H5A · · · O16B [(c)]	0.93	2.45	3.242 (3)	144
C9A – H9A · · · O16A ∗	0.93	2.46	2.777 (3)	100
C9A – H9A · · · O16B [(c)]	0.93	2.47	3.279 (3)	145
C9B – H9B · · · O16B ∗	0.93	2.44	2.759 (3)	100

∗Intramolecular hydrogen bond interactions.Symmetry codes: *(a) 1 − x, −y, 1 − z.*(b) *−x, −y, −z.*(c) *x*, 1/2 − *y*, 1/2 +*z.*

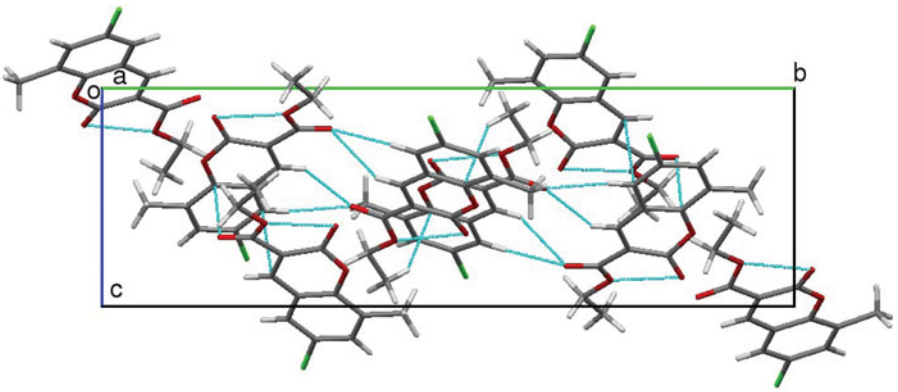

Figure 5. Packing of molecules when viewed along *a*-axis.

123.11(19)° and 123.24(19)° for C5-C6-C9 of molecules A and B, respectively. Generally, these values are respectively smaller and greater than 120° for coumarin derivatives. All these features are commonly found in coumarin derivatives and are also observed in the title compound.

The widening of the angles O13-C11-C10 in molecules A and B are, respectively, 127.7(2)° and 128.2(2)°. This is attributed to the lone-pair interactions between O13-O12 [13].

The torsion angles of molecules A and B (C11-C10-C14-C16) are, respectively, −167.7(2)° and 174.9(2)°, which indicate no significant change with the substitution of carboxylic group at C10 position. This is comparable to the substitution of carboxylic group at the same position reported earlier [11,12].

Packing of the molecules in the unit cell down the *a* and *c*-axes are as shown in the Figs. 5 and 6.

There are two intramolecular hydrogen bonds C9-H9-O16. The packing diagrams of the molecules indicate the contact between the methyl group attached to phenoxy moiety and the pyrone ring.

In vitro antibacterial activity

The results of antibacterial activity of the title compound is as shown in the Table 6. The antibacterial screening revealed that the compound shows lesser or average activity against various bacterial strains. The synthesized compound showed better inhibition against a gram-negative bacterium, *S. typhimurium.*

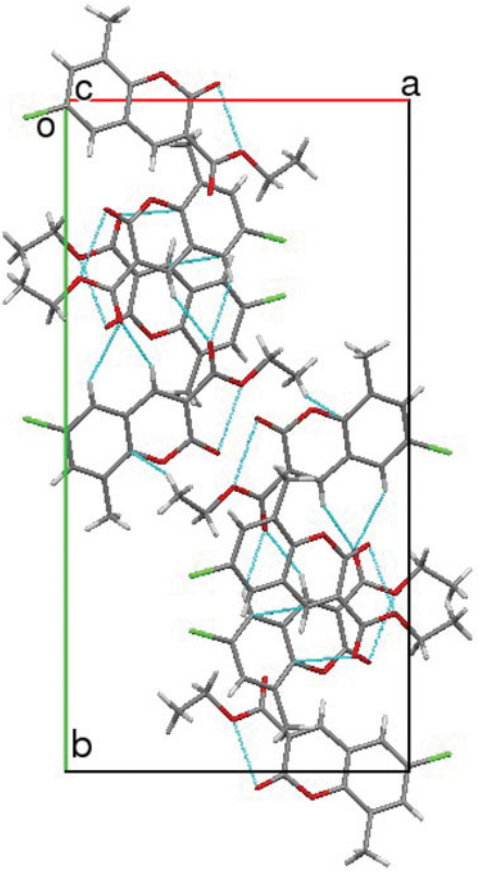

Figure 6. Packing of molecules when viewed along *c*-axis.

Table 6. MIC of the titled compound against various bacterial strains.

Bacterial Strains	MIC (mg/mL)
Bacillus cereus	0.25
Staphylococcus aureus	0.125
Salmonella typhimurium	0.03125
Pseudomonas aeruginosa	0.25

Acknowledgments

The authors are thankful to IoE, Vijnana Bhavan, University of Mysore, Mysuru for providing the single-crystal X-ray diffraction facility and to Prof. V. Ravishankar Rai and Manasa Ravindra Walmiki, Department of Studies in Microbiology, University of Mysore, Manasagangotri, Mysuru, for assistance in evaluating biological activity. NLR is thankful to UGC, New Delhi for RFSMS fellowship. SAK and PT acknowledge the financial support provided by the VGST, Bengaluru, and UGC, New Delhi, and to the Principal of Yuvaraja's College and National Institute of Engineering, Mysuru.

References

[1] Neyts, J., De Clercq, E., Singha, R., Hsiung Chang, Y., & Das, A. R. *et al.* (2009). *J. Med. Chem.*, *52*, 1486–1490.
[2] Zavrsnik, D., Spirtovic-Halilovic, S., & Softic, D. (2011). *Period. Biol.*, *113*, 93–97.
[3] Kharb, R., Kaur, M., & Sharma, A. K. (2013). *Int. I. Pharm. Sci. Rev.*, *20*(1), 87–94.
[4] Jung, J-C., & Park, O-S. (2009). *Molecules*, *14*, 4790–4803.
[5] Klancnik, A., Piskernik, S., Jersek, B., & Mozina, S. S. (2010). *J. Microbiol. Methods.*, *81*, 121–126.
[6] Elkhair, E. A., Hussein, F., & Mohsen, U. A. (2010). *Journal of Al -Azhar University-Gaza (ICBAS Special Issue)*, *12*, 45–54.
[7] Bruker, APEX2, SAINT, & SADABS. (2009). Bruker AXS Inc.: Madison, Wisconsin, USA.
[8] Sheldrick, G. M. (2008). *Acta Cryst.*, *A64*, 112.
[9] Spek, A. L. (1990). *Acta Cryst.*, *A46*, 34.
[10] Macrae, C. F., Bruno, I. J., Chisholm, J. A., Edgington, P. R., McCabe, P. et al. (2008). *J. Appl. Cryst.*, *41*, 466.
[11] Santos-Contreras, R. J., Martinez-Martinez, F. J., Garcia-Baez, E. V., Padilla-Martinez, I. I., Peraza, A. L., & Herbert, H. (2007). *Acta Cryst.*, *C63*, o239–o242.
[12] Xu, C-L., Yang, N., Guo-Yu, Y., Su-Fang, F., & Cao-Yuan, N. (2009). *Acta Cryst.*, *E65*, o2991.
[13] Basanagouda, M., Kulkarni, M. V., Sharma, D., & Gupta, V. K. (2011). *J. Chem. Crystallogr.*, *41*, 541–544.